



ELSEVIER

Available online at www.sciencedirect.com

SCIENCE @ DIRECT®

Progress in Biophysics and Molecular Biology 90 (2006) 186–206

www.elsevier.com/locate/pbiomolbio

Progress in
Biophysics
& Molecular
Biology

Review

Role of stretch-activated channels on the stretch-induced changes of rat atrial myocytes

Jae Boum Youm^a, Jin Han^a, Nari Kim^a, Yin-Hua Zhang^b, Euiyong Kim^a, Hyun Joo^a, Chae Hun Leem^c, Sung Joon Kim^d, Kyung A Cha^d, Yung E. Earm^{d,*}

^a*Mitochondrial Signaling Laboratory, Department of Physiology and Biophysics, College of Medicine, Cardiovascular and Metabolic Disease Center, Biohealth Products Research Center, Inje University, Busan 614-735, Republic of Korea*

^b*Department of Cardiovascular Medicine, University of Oxford, John Radcliffe Hospital, Oxford, UK*

^c*Department of Physiology and the Institute for Calcium Research, University of Ulsan College of Medicine, Songpaju, Seoul 138-736, Republic of Korea*

^d*Department of Physiology and National Research Laboratory for Cellular Signalling, Seoul National University College of Medicine, 28 Yonkeun-Dong, Chongno-Ku, 110-799, Seoul, Republic of Korea*

Available online 7 July 2005

Abstract

The role of stretch-activated channels (SACs) on the stretch-induced changes of rat atrial myocytes was studied using a computer model that incorporated various ion channels and transporters including SACs. A relationship between the extent of the stretch and the activation of SACs was formulated in the model based on experimental findings to reproduce changes in electrical activity and Ca^{2+} transients by stretch. Action potentials (APs) were significantly changed by the activation of SACs in the model simulation. The duration of the APs decreased at the initial fast phase and increased at the late slow phase of repolarisation. The resting membrane potential was depolarised from -82 to -70 mV. The Ca^{2+} transients were also affected. A prolonged activation of SACs in the model gradually increased the amplitude of the Ca^{2+} transients. The removal of Ca^{2+} permeability through SACs, however, had little effect on the stretch-induced changes in electrical activity and Ca^{2+} transients in the control condition. In contrast, the removal of the Na^{+} permeability nearly abolished these stretch-induced changes. Plotting the peaks of the Ca^{2+} transients during the activation of the SACs along a time axis revealed that they follow the time course of

*Corresponding author. Tel.: +82 2 740 8224; fax: +82 2 763 9667.

E-mail address: earmye@snu.ac.kr (Y.E. Earm).

the Na_i^+ concentration. The Ca^{2+} transients were not changed when the Na_i^+ concentration was fixed to a control value (5.4 mM). These results predicted by the model suggest that the influx of Na^+ rather than Ca^{2+} through SACs is more crucial to the generation of stretch-induced changes in the electrical activity and associated Ca^{2+} transients of rat atrial myocytes.

© 2005 Elsevier Ltd. All rights reserved.

Keywords: Mechano-electric feedback; Stretch-activated channels; Stretch; Rat atrial myocytes

Contents

1. Introduction	187
2. Methods	188
2.1. Cell preparation	188
2.2. Solutions	189
2.3. Electrophysiological recordings	189
2.4. Application of stretch	189
2.5. Mathematical model	189
2.5.1. Stretch-activated non-selective cation channels (SACs) in the model	190
2.5.2. Background non-selective cation channels in the model	191
2.5.3. Model formulations for the inward rectifier K^+ current (I_{K1})	191
2.5.4. Model formulations for the depolarisation-activated outward K^+ current ($I_{\text{k,out}}$)	191
2.5.5. Constant field equations	192
3. Results	192
3.1. Reconstruction of whole-cell membrane currents of rat atrial myocytes	192
3.2. Stretch-induced changes in I – V relationship	193
3.3. Stretch-induced changes in AP	195
3.4. Stretch-induced changes in Ca^{2+} transients	195
4. Discussion	198
Editor's note	202
Acknowledgements	202
Appendix	202
References	203
Further reading	206

1. Introduction

Mechanical stimulation such as stretch or dilation of the heart is known to modulate the electrical activity of myocytes, which suggests that there is a feedback system in the heart, in addition to excitation–contraction coupling, whereby mechanical stimuli modulate electrical activity (Lab, 1982; Nazir and Lab, 1996). This feedback system is often referred to as mechano-electric feedback (Lab, 1996; Kohl and Ravens, 2003). The stretch-induced modulation of electrical activity includes after-depolarisation (Lab, 1978; Franz et al., 1989; Hansen, 1993), depolarisation of the resting potential (Boland and Troquet, 1980; Franz et al., 1992) and alteration of the action potential (AP) duration (Dean and Lab, 1989; Franz et al., 1989; Taggart, 1996). In severe cases, these changes are found to be arrhythmogenic. There is an increasing body of evidence that major events of mechano-electric feedback are mediated by the activation of stretch-activated channels (SACs) (Bustamante et al., 1991; Craelius, 1993; Hoyer et al., 1994;

Kiseleva et al., 2000). In other words, SACs may act as a sensor or transducer of mechano-electric feedback. There is also evidence that myocardial stretch modulates $[Ca^{2+}]_i$ (Allen and Kurihara, 1982; Hongo et al., 1996; Calaghan et al., 2003). Changes in $[Ca^{2+}]_i$ are associated with the slow response: the secondary, slower increase in force that occurs after an immediate increase in force by myocardial stretch. The opening of SACs is often used to explain this effect (Tavi et al., 1998; Calaghan et al., 2003). As an alternative mechanism, the autocrine–paracrine effect involving the Na^+/H^+ exchanger activation (Alvarez et al., 1999; Perez et al., 2001) or nitric oxide (NO) release (Petroff et al., 2001; Casadei and Sears, 2003) has been suggested to mediate the slower increase in force by myocardial stretch.

We previously described the effects of stretch on the electrical activity of rat atrial myocytes (Zhang et al., 2000). In that study, we used two microelectrodes to mechanically stretch the atrial myocytes, leading to depolarisation of the resting membrane potential and prolongation of the AP duration, both of which are mediated by the activation of SACs that have non-selective permeability to various cations. However, the physiological role of each cation in the stretch-induced changes in electrical activity is very hard to predict or determine with the limited results of stretch experiment. Recently, Dr. A. Noma's group developed a cardiac cell model (Kyoto model) to describe the electrical activity, Ca^{2+} transients, and contractile force in guinea-pig sino-atrial node cells and ventricular myocytes (Matsuoka et al., 2003; Sarai et al., 2003). A modification of the Kyoto model allowed us to simulate the electrical activity and Ca^{2+} transients of rat atrial myocytes (see Methods). Combining the modified Kyoto model and quantitative results of our study on SACs (Zhang et al., 2000), we were able to simulate the effect of stretch on the electrical activity and Ca^{2+} transients. The simulated APs and Ca^{2+} transients are significantly changed with increasing conductance of SACs in the model, and these results corresponded well with our previous experimental finding. In addition to that comparison and because SACs are permeable to both Na^+ and Ca^{2+} (Sachs, 1988; Kim, 1993), we were prompted to investigate whether Na^+ or Ca^{2+} ion permeability is more important in the development of the stretch-induced changes in electrical activity and Ca^{2+} transients in rat atrial myocytes.

2. Methods

2.1. Cell preparation

The investigation conformed to the guidelines provided by the Committee for Animal Experiment of the College of Medicine, Seoul National University. Young adult Sprague-Dawley rats (200–250 g) were killed by cervical dislocation. The hearts were isolated and perfused with 100 ml of oxygenated normal Tyrode solution (37 °C). The perfusion solution was changed to 50 ml of nominally Ca^{2+} -free Tyrode solution, and then to the same solution containing 0.12 mg ml^{-1} collagenase (Yakult, Japan) and $50 \mu\text{M}$ $CaCl_2$. After 14 min, the hearts were removed from the Langendorff apparatus and placed in a high- K^+ , low- Cl^- storage medium. The atria and their appendages were dissected into small pieces and mechanically dispersed with a fire-polished Pasteur pipette in the same solution. Isolated myocytes were stored in the high- K^+ , low- Cl^- storage medium at 4 °C until use.

2.2. Solutions

The high- K^+ , low- Cl^- storage medium contained (in mM) 50 L-glutamate, 50 KCl, 20 taurine, 20 KH_2PO_4 , 3 $MgCl_2$, 10 glucose, 10 *N*-[2-hydroxyethyl]piperazine-*N'*-[2-ethanesulfonic acid] (HEPES), 0.5 ethyleneglycol-bis(β -aminoethyl ether)-*N,N,N',N'*-tetraacetic acid (EGTA); the pH was adjusted to 7.3 with KOH. For the perfusion of myocytes during the electrophysiological recordings, a normal Tyrode external solution and high K^+ (140 KCl) pipette solution were used. The normal Tyrode solution contained (in mM): 143 NaCl, 5.4 KCl, 0.5 $MgCl_2$, 1.8 $CaCl_2$, 5.5 glucose, and 5 HEPES (pH 7.4). The external Cs^+ solutions contained (in mM): 140 CsCl, 2 $MgCl_2$ and 10 HEPES (pH 7.4), and the internal Cs^+ solution contained 140 CsCl, 1 $MgCl_2$, 10 HEPES, 5 EGTA, 5 MgATP, 2.5 ditris-phosphocreatine and 2.5 disodium phosphocreatine (pH 7.2). The external and internal Na^+ solutions were made by replacing 140 mM CsCl with 140 mM NaCl. Unless otherwise noted, all chemicals were purchased from Sigma (St. Louis, MO, USA).

2.3. Electrophysiological recordings

The standard whole-cell voltage clamp method (Hamill et al., 1981) was performed using an Axopatch-1C amplifier (Axon Instruments, CA, USA). The recording pipettes were fabricated and fire-polished from 1.5 mm o.d. glass (Clark Electromedical, UK) to produce microelectrodes with resistances of 2–4 M Ω when filled with a K^+ -rich recording solution. A gigaseal was made by applying negative pressure at approximately –10 mmHg, and seal resistance was usually above 2 G Ω . The current signals were filtered via a 1–10 kHz, 4-pole Bessel-type low-pass filter and digitised using Digidata 1200 (Axon Instruments) for subsequent analysis (pCLAMP software, version 6.0.1, Axon Instruments). In most experiments, the temperature was set at room temperature (20–24 °C). All averaged and normalised data are presented as means \pm S.E.M. The reversal potentials were determined in each cell as the zero current intercept of the polynomial fit (4-order) to the current–voltage relationship.

2.4. Application of stretch

The stretch was achieved by displacing two microelectrodes attached to the ends of atrial myocytes (Zhang et al., 2000). The extent of the stretch was expressed as the percentile change in cell length relative to the original cell length:

$$\Delta L = (L_{\text{stretch}} - L_{\text{original}}) / L_{\text{original}} \times 100. \quad (1)$$

2.5. Mathematical model

The model of stretch-induced changes in electrical activity used in this study was based on the Kyoto model (Matsuoka et al., 2003; Sarai et al., 2003), and it can reproduce and describe the various cellular activities of cardiomyocytes such as AP, sarcoplasmic reticulum (SR) Ca^{2+} dynamics, and cell contraction. In order to reproduce these activities, the model incorporated ion channels, exchangers, pumps, Ca^{2+} -binding proteins, SR compartment, and contractile apparatus. The Kyoto model was originally developed to fit the experimental findings on the guinea-pig sino-atrial node cells and ventricular myocytes. The improvement of the Kyoto model

compared with the Oxsoft or Luo-Rudy model can be summarised as follows: (1) The $\text{Na}^+/\text{Ca}^{2+}$ exchanger, Na^+/K^+ pump, and SR Ca^{2+} pump are all described with the lumped two-state model. (2) The recent experimental data on the background non-selective cation channels (Zhang et al., 2000) are included. (3) The Ca^{2+} -mediated inactivation and Ca^{2+} -induced activation of the ryanodine receptor channel are calculated. (4) The presence of common equations between the sinoatrial node cell and ventricular cell makes it easy to compare them and develop another cell model including atrial cell model. We had to make some species-specific modifications because our experimental findings on the stretch-induced electrical activity were mainly obtained from rat atrial myocytes. The ionic currents through the inward rectifier K^+ channel (I_{K1}) and depolarisation-activated outward K^+ channel ($I_{\text{K,out}}$) were modified to fit the experimental results of our voltage clamp study in rat atrial myocytes. The volumes of the cell were adjusted to approximate those of the rat atrial myocytes. The ionic concentrations were also modified to be the same as those used in our experimental work. In order to simulate the stretch-induced effects, we also introduced the terms of SACs. There is a growing body of evidence that a stretch of cardiomyocytes also activates the K^+ -selective TREK (Terrenoire et al., 2001; Niu and Sachs, 2003) and swelling-activated Cl^- -selective (Sorota, 1992; Tseng, 1992; Vandenberg et al., 1994) channels. However, the mode of stretch activating the channels is usually different from that of SACs, which are activated by a stretch along the longitudinal axis. The stretch-sensitive TREK and swelling-activated Cl^- -selective channels have been found to be activated by applying a negative pressure to the membrane patch and perfusing a hypoosmotic solution to the cell, respectively. As we simulate the effects of a stretch along the longitudinal axis, only the SACs were incorporated into the model.

2.5.1. Stretch-activated non-selective cation channels (SACs) in the model

The amplitude of I_{SAC} in rat atrial myocytes can be determined by the following equation with a slight modification from the previous model (Sachs, 1994):

$$I_{\text{SAC}}/I_{\text{SAC,max}} = 1/(1 + \exp((\Delta L - \Delta L_{1/2})/(-s))), \quad (2)$$

where I_{SAC} is defined as the current density (pA/pF) at each degree of direct stretch. $I_{\text{SAC,max}}$ is defined as the current density at maximum stretch without cell death or breakdown of the seal. ΔL is the percentile change in cell length, which was already described in Eq. (1). $\Delta L_{1/2}$ is the ΔL where the I_{SAC} reaches half the amplitude of $I_{\text{SAC,max}}$. The s represents the slope factor describing the stretch sensitivity. Fitting the I_{SAC} -stretch relationship in our previous study (Zhang et al., 2000) to Eq. (2) gives the values of 16.9% and 6.3% corresponding to $\Delta L_{1/2}$ and s , respectively. The amplitude can be expressed simply as the function of permeability and the constant field equations for each ion species without considering the voltage-dependent gating of channels because I_{SAC} shows linear voltage dependence (Zhang et al., 2000). From the reversal potential ($V_{\text{rev}} = -6.1$ mV) in the presence of a physiological salt solution, it was calculated that the permeability ratio of $P_{\text{Na}}:P_{\text{K}}$ was 1:1.32. The permeability ratio was then used in the model to calculate the fluxes of each cation by the activation of I_{SAC} . The permeability ratio of $P_{\text{Na}}:P_{\text{Ca}}$ (1:0.7) was obtained by fitting the results from Kim (1993). The SACs have been known to have a time-dependent behaviour, a transient activation during a sustained stretch (Hu and Sachs, 1996). Our experimental results (Zhang et al., 2000) also demonstrate that the activation of SACs is transient with a sustained stretch. Although the activation is transient, it was static or growing at

least 1 min of stretch (see Fig. 2A). Therefore, we assumed that the increase in SACs conductance is statically active during a short period of stretch (<30 s) in the modelling.

2.5.2. Background non-selective cation channels in the model

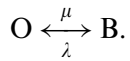
Under the whole-cell voltage clamp, the replacement of Na^+ with NMDG^+ significantly reduced the membrane conductance in rat atrial myocytes (Youm et al., 2000). This conductance still remained after blocking the time- and voltage-dependent ion channels under an isotonic Na^+ condition. Although it showed a non-selective permeability over the various cations, the permeability ratio ($P_{\text{Cs}}:P_{\text{Na}}:P_{\text{Li}} = 1.49:1:0.70$) was different from that of I_{SAC} ($P_{\text{Cs}}:P_{\text{Na}}:P_{\text{Li}} = 1.05:1:0.98$) (Zhang et al., 2000). This conductance was described in the model as a sum of cation components according to their relative permeability ratios.

2.5.3. Model formulations for the inward rectifier K^+ current (I_{K1})

State C goes into state O reversibly



State O also goes into state B reversibly



$$I_{\text{K1}} = 43.2(V - E_{\text{K}})([\text{K}^+]_{\text{o}}/5.4)^{0.62}nf_{\text{U}}, \quad (3)$$

$$E_{\text{K}} = -86.7([\text{K}^+]_{\text{i}} = 140 \text{ mM}, [\text{K}^+]_{\text{o}} = 5.4 \text{ mM}), \quad (4)$$

$$\alpha_n = 1.0/(8000 \exp((V - E_{\text{K}} - 97)/8.5) + 7 \exp((V - E_{\text{K}} - 97)/300)), \quad (5)$$

$$\beta_n = 1.0/(0.00014 \exp((V - E_{\text{K}} - 97)/(-9.1)) + 0.2 \exp((V - E_{\text{K}} - 97)/(-500))), \quad (6)$$

$$\mu = 12.75 \exp(0.035(V - E_{\text{K}} - 10))/(1 + \exp(0.015(V - E_{\text{K}} - 140))), \quad (7)$$

$$\lambda = 3 \exp(-0.048(V - E_{\text{K}} - 10)) \times (1 + \exp(0.064(V - E_{\text{K}} - 38)))/(1 + \exp(0.03(V - E_{\text{K}} - 70))), \quad (8)$$

$$f_{\text{B}} = \mu/(\mu + \lambda), \quad (9)$$

$$f_{\text{U}} = \lambda/(\mu + \lambda). \quad (10)$$

2.5.4. Model formulations for the depolarisation-activated outward K^+ current ($I_{\text{k,out}}$)

$$I_{\text{K,out}} = I_{\text{K,fast}} + I_{\text{K,slow}}, \quad (11)$$

$$I_{\text{K,fast}} = I_{\text{K,fast}}\text{K} + I_{\text{K,fast}}\text{Na}, \quad (12)$$

$$I_{\text{K,fast}}\text{K} = 2.9mh\text{K}_{\text{CF}}, \quad (13)$$

$$I_{\text{K,fast}}\text{Na} = 0.26mh\text{Na}_{\text{CF}}, \quad (14)$$

$$\alpha_m(I_{K,\text{fast}}) = 1/(1.4 \exp(V/(-14241)) + 0.35 \exp(V/(-15))), \quad (15)$$

$$\beta_m(I_{K,\text{fast}}) = 1/(22.7 \exp(V/37.9) + 1775 \exp(V/8.4)), \quad (16)$$

$$\alpha_h(I_{K,\text{fast}}) = 1/(2.5 \exp(V/3.2) + 2195 \exp(V/23.6)), \quad (17)$$

$$\beta_h(I_{K,\text{fast}}) = 1/(40.4 \exp(V/(-76022)) + 0.29 \exp(V/(-5.4))), \quad (18)$$

$$I_{K,\text{slow}} = I_{K,\text{slow}}K + I_{K,\text{slow}}Na, \quad (19)$$

$$I_{K,\text{slow}}K = 1.8mhK_{CF}, \quad (20)$$

$$I_{K,\text{slow}}Na = 0.16mhNa_{CF}, \quad (21)$$

$$\alpha_m(I_{K,\text{slow}}) = 1/(0.0002 \exp(V/(-7.2)) + 1.37 \exp(V/(-47.8))), \quad (22)$$

$$\beta_m(I_{K,\text{slow}}) = 1/(1346 \exp(V/16.0) + 1600 \exp(V/11.3)), \quad (23)$$

$$\alpha_h(I_{K,\text{slow}}) = 1/(6613 \exp(V/135222) + 143392 \exp(V/12.1)), \quad (24)$$

$$\beta_h(I_{K,\text{slow}}) = 1/(4801 \exp(V/(-125)) + 119 \exp(V/(-10.3))). \quad (25)$$

2.5.5. Constant field equations

$$K_{CF} = \frac{FV}{RT} \frac{[K^+]_i - [K^+]_o \exp(-FV/RT)}{1 - \exp(-FV/RT)}, \quad (26)$$

$$Na_{CF} = \frac{FV}{RT} \frac{[Na^+]_i - [Na^+]_o \exp(-FV/RT)}{1 - \exp(-FV/RT)}, \quad (27)$$

$$Ca_{CF} = \frac{2FV}{RT} \frac{[Ca^{2+}]_i - [Ca^{2+}]_o \exp(-2FV/RT)}{1 - \exp(-2FV/RT)}. \quad (28)$$

3. Results

3.1. Reconstruction of whole-cell membrane currents of rat atrial myocytes

The building of a computer model based on experimental findings is a prerequisite for the simulation or prediction of physiological phenomena such as membrane excitability, transport, and contractility. Based on the Kyoto model, we were able to make a computer model of rat atrial myocytes demonstrating stretch-induced changes in electrical activity and Ca^{2+} transients with some modifications to fit our experimental results (see Methods). In order to check the validity of our model, we measured whole-cell membrane currents elicited by varying voltage steps or ramp pulses and compared them with those from the model simulation. Fig. 1A illustrates a typical series of whole-cell membrane currents of rat atrial myocytes activated by voltage steps between -120 and $+100$ mV from a holding potential of -80 mV. In response to hyperpolarising voltage

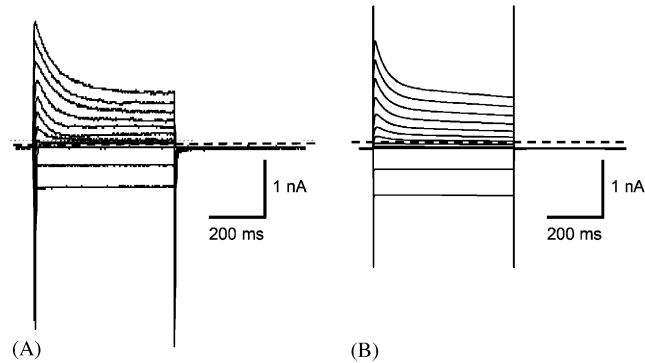


Fig. 1. Comparison of voltage clamp recordings from a single rat atrial myocyte with those in the model simulation. (A) Experimental recordings on voltage steps to -120 to $+100$ mV from a holding potential of -80 mV. The duration of the voltage steps is 500 ms and the interval is 10 s. (B) Current recordings from voltage steps by model simulation.

steps, large sustained inward currents appeared, whereas depolarisation up to -20 mV induced very small steady-state outward currents, which are known characteristics of inward rectifier K^+ channels in cardiac myocytes. From -60 mV, capacitive-like transient inward currents were also noticed, which represent the activation of voltage-gated Na^+ channels. From -20 mV, time-dependent outward currents became dominant. These currents represent the currents carried by depolarisation-activated outward K^+ channels. The depolarisation-activated outward K^+ current is the main repolarisation-inducing current in rat atrial myocytes (Boyle and Nerbonne, 1992). As illustrated in Fig. 1B, the recording of the model simulation elicited by voltage steps faithfully reproduced the typical time-dependent membrane currents in rat atrial myocytes (see Fig. 1A).

3.2. Stretch-induced changes in $I-V$ relationship

In a second series of experiments, the effects of stretch on the $I-V$ relationship were examined. Mechanical stimuli that have been used at the single-cell level include osmotic swelling, positive inflation pressure, mechanical indentation, and uniaxial stretch (Cazorla et al., 1999; Riemer and Tung, 2003). We chose uniaxial stretch to examine the effects of stretch on the $I-V$ relationship because it is generally assumed to be the most appropriate model analogous to the stretch of tissue (Brady, 1991).

The atrial cells were dialysed with a high KCl pipette solution, and the membrane voltage was held at -30 mV. To obtain the brief current–voltage relationships ($I-V$ curves), ramp pulses were applied every 20 s (see the original chart trace in Fig. 2A). The $I-V$ curves were obtained in control conditions and during the application of stretch (20% stretch) and compared between the experimental (Fig. 2A, control) and simulation recordings (Fig. 2B, control). The control $I-V$ curves obtained in both conditions showed strong inward rectification and outward rectification was also noticeable from the membrane potential of 0 mV. The reversal potentials ranged between -80 and -65 mV. A uniaxial stretch of single atrial myocytes (20% increase in length) consistently increased the membrane conductance and shifted the reversal potential to the positive direction (Fig. 2A, stretch). The difference between the currents before and after the stretch was

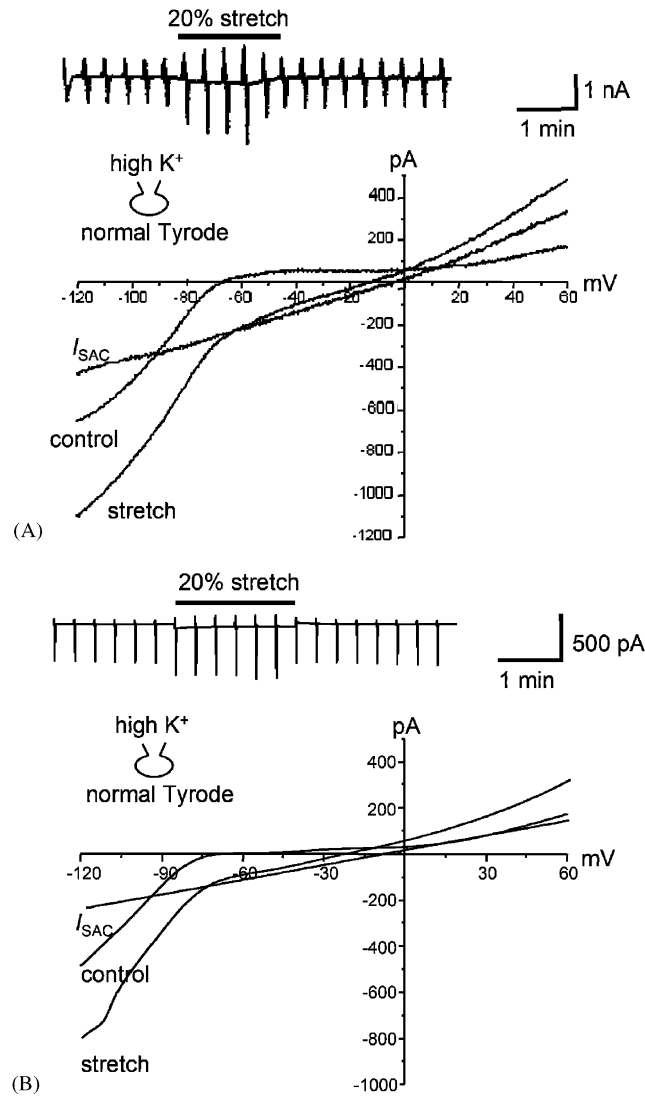


Fig. 2. Experimental recordings showing the effect of stretch on the I - V relationship. (A) The effect of direct stretch by two microelectrodes on the I - V relationship. In order to get an I - V relationship, ramp pulses from -120 to $+60$ mV with dV/dt of -225 mV s⁻¹ were applied to the cell every 20 s. The holding potential between ramp pulses was -30 mV. The left upper inset shows the chart recording of current traces before, during, and at recovery of stretch (20%) in normal Tyrode external and high K⁺ internal solution. The lower inset shows the I - V relationship obtained from the left upper inset before and during stretch. (B) Simulation recordings of current traces and I - V relationship before and during stretch. Pulse protocols and ionic concentrations are the same as those in A. The activation of SACs was determined by Eq. (2) (see Methods for details).

obtained by digital subtraction and was regarded as the stretch-activated current (I_{SAC}). The reversal potential of I_{SAC} was -6.1 ± 3.7 mV ($n = 7$). The P_{Na}/P_K was found to be 0.76, as calculated from the value of the reversal potential (-6.1 mV) under physiological ionic condition. A simulation model of the stretch was developed with the formulation and incorporation of SACs

into our computer model using quantitative data such as the permeability ratio, voltage-, and stretch-dependence obtained from our experimental results (see Methods). As illustrated in Fig. 2B, the model simulation faithfully reproduced the experimental results in Fig. 2A. The activation of SACs in the model simulation increased the whole-cell membrane currents and shifted the reversal potential to the positive direction.

3.3. Stretch-induced changes in AP

The stretch of cardiomyocytes along the longitudinal axis has been shown to depolarise the diastolic membrane (Hansen et al., 1991; Kohl et al., 1999; Zhang et al., 2000). However, the effect on the AP duration (APD) is variable: decrease (White et al., 1993; Tung and Zou, 1995) or increase (Zeng et al., 2000) in APD. We performed stretch experiments using our simulation model and compared them with experimental results. As the amplitude of I_{SAC} was increased by a virtual stretch, the diastolic membrane of the model cell was depolarised in a stretch-dependent manner. If the increase in the conductance of SACs was sufficient, the depolarisation reached a threshold that resulted in the firing of APs (Fig. 3B). Stretch-induced APs had longer duration than electrically generated APs, but the amplitude of stretch-induced APs was slightly decreased, possibly via partial inactivation of sodium channels during the slow depolarisation to the threshold level. The model agreed well with our previous data (Zhang et al., 2000) that showed a stretch (20%) generated APs without electrical stimulation (Fig. 3A). The APD during the stretch was also significantly changed in opposite directions at different levels of repolarisation. The APD at a 90% repolarisation level (APD_{90}) was increased from 73.8 to 123.1 ms by a 10% stretch, while the APD at a 20% repolarisation level (APD_{20}) was decreased from 4.6 to 4.0 ms (Fig. 3C). Comparing the APD between stretches of 10% and 20%, the APD of 20% stretch was significantly decreased (data not shown; $\text{APD}_{20} = 3.57$ ms, $\text{APD}_{90} = 54.9$ ms), possibly via partial inactivation of the L-type Ca^{2+} current secondary to the severe degree of depolarisation (resting membrane potential = -53.2 mV).

The activation of SACs would increase the membrane permeability for both Na^+ and Ca^{2+} because SACs are non-selective to cations (Kim, 1993). However, the prediction or determination of the differential effects of increased permeability of each ion species through SACs under physiological ionic conditions is improbable because of the technical difficulty. By using the simulation models, we could circumvent the technical difficulty that is expected in real experiments; thus, we decided to investigate whether one of the ion species (i.e., Na^+ or Ca^{2+}) plays a more essential role in the stretch-induced modulation of electrical activity in atrial myocytes. We tested two different cases in which permeability to one of the ions through SACs was set to 0. As shown in Fig. 4B, reducing the Ca^{2+} permeability to 0 from control failed to significantly affect the stretch-induced changes in the AP (Fig. 4A). On the other hand, reducing the Na^+ permeability nearly abolished the stretch-induced changes in the AP under a control condition (Fig. 4C).

3.4. Stretch-induced changes in Ca^{2+} transients

The evidence that myocardial stretch modulates $[\text{Ca}^{2+}]_i$ exists (Allen and Kurihara, 1982; Hongo et al., 1996; Tavi et al., 1998; Calaghan et al., 2003). The opening of SACs is often

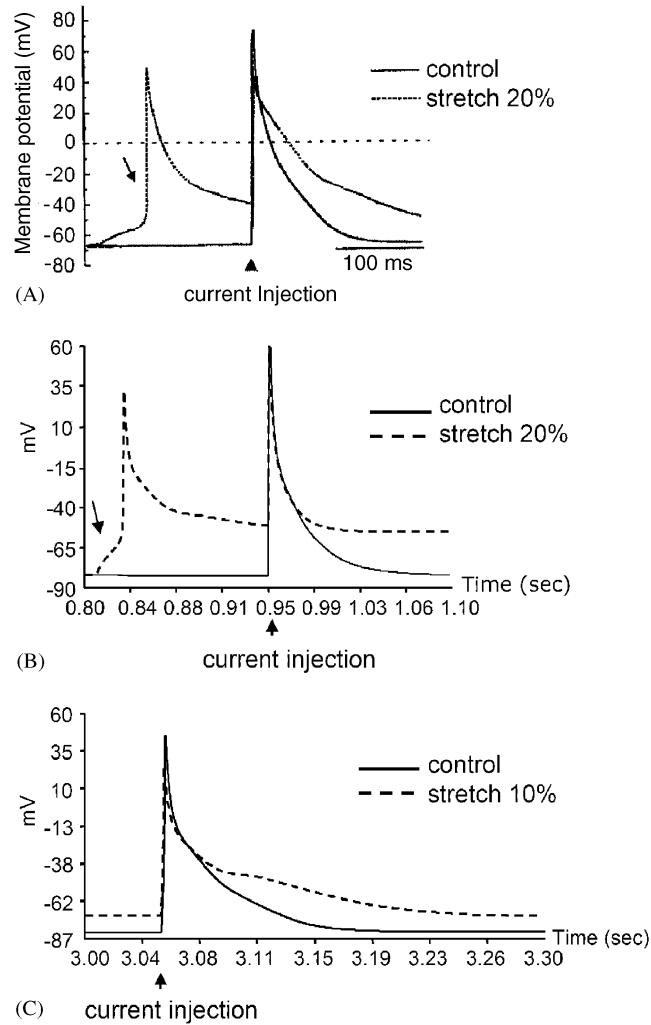


Fig. 3. Comparison of the effects of direct stretch on the membrane potentials by experimental findings with those by model simulation. (A) The effects of direct stretch (20%) on the diastolic membrane potential and AP obtained experimentally. The direct stretch depolarised the diastolic membrane and triggered an AP (arrow) without an electrical stimulus. The duration of the AP triggered by a current injection (upward triangle) was prolonged by the stretch compared with the control. Reproduced with the permission of Zhang et al. (2000). (B) The effects of the direct stretch on the diastolic membrane potential and the AP in a model simulation. (C) Comparison of APs between the control and the 10% stretch in a model simulation. The model simulation depolarised the diastolic membrane (from -82 to -70 mV at) and prolonged the APD at a 90% repolarisation level (from 73.8 to 123.1 ms).

suggested as a possible mediator of the stretch-induced changes in Ca^{2+} transients (Tavi et al., 1998; Calaghan et al., 2003). Fig. 5A illustrates the model-predicted effects of stretch on the Ca^{2+} transients. A simulated stretch gradually increased the amplitude of the Ca^{2+} transients as well as the diastolic $[\text{Ca}^{2+}]_i$ (Fig. 5A). The release of the stretch slowly reversed the stretch-induced changes to the control level.

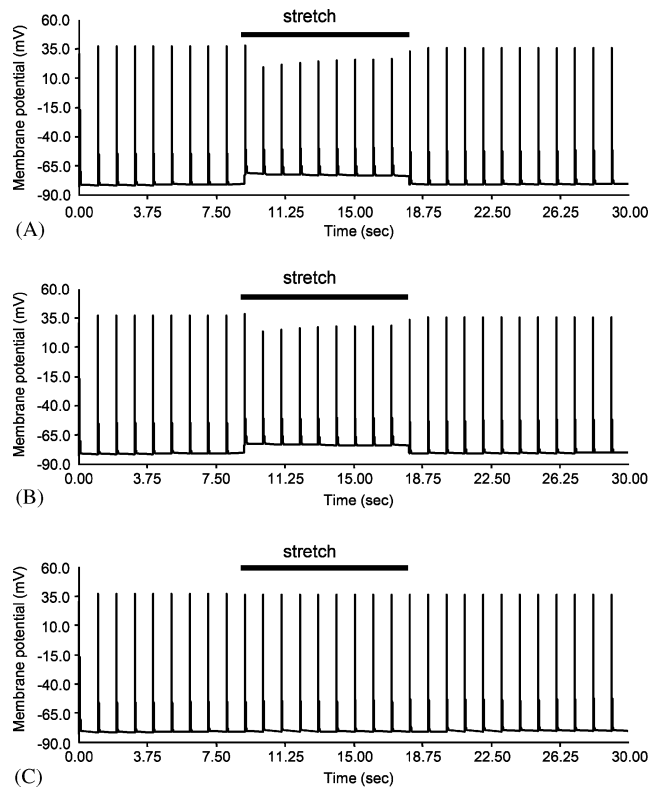


Fig. 4. Model predictions of the AP changes by activation of SACs (corresponding to a 10% stretch) with different ionic permeabilities. (A) A prediction of changes in APs when $P_{\text{Na}}:P_{\text{K}}:P_{\text{Ca}}$ through SACs is 1:1.32:0.70. (B) A prediction of changes in APs when P_{Ca} is 0 ($P_{\text{Na}}:P_{\text{K}}:P_{\text{Ca}} = 1:1.32:0$). (C) A prediction of changes in APs when P_{Na} is 0 ($P_{\text{Na}}:P_{\text{K}}:P_{\text{Ca}} = 0:1.32:0.7$). The stimulus interval was 1.0 s.

With regard to the APs, it was suggested that the permeability to Na^+ rather than Ca^{2+} plays a more crucial role in the stretch-induced modulation of electrical activity in atrial myocytes (Fig. 4). As for which ion species plays a more crucial role in the generation of the gradual increase in the amplitude of Ca^{2+} transients during the stretch, Fig. 5B shows that reducing the Ca^{2+} permeability has little effect on the stretch-induced changes in the Ca^{2+} transients. On the other hand, reducing the Na^+ permeability nearly abolished the stretch-induced changes (Fig. 5C), which contradicts the possibility that the Ca^{2+} influx through SACs could directly increase the amplitude of Ca^{2+} transients during a stretch. As an alternative mechanism, an indirect pathway of Ca^{2+} influx could be proposed. The activation of SACs should increase $[\text{Na}^+]_i$ because the channels are permeable to Na^+ as well as Ca^{2+} (Kim, 1993). The accumulation of Na^+ could then lead to the upregulated operation of the $\text{Na}^+/\text{Ca}^{2+}$ exchanger in reverse-mode during the rising phase of the APs, which finally would increase the Ca^{2+} influx. In support of this possibility, the sustained activation of SACs by a virtual stretch gradually increased $[\text{Na}^+]_i$ while the release of the stretch very slowly reversed $[\text{Na}^+]_i$ in the model simulation (Fig. 6A). Interestingly, the peaks of the Ca^{2+} transients during the stretch along a time

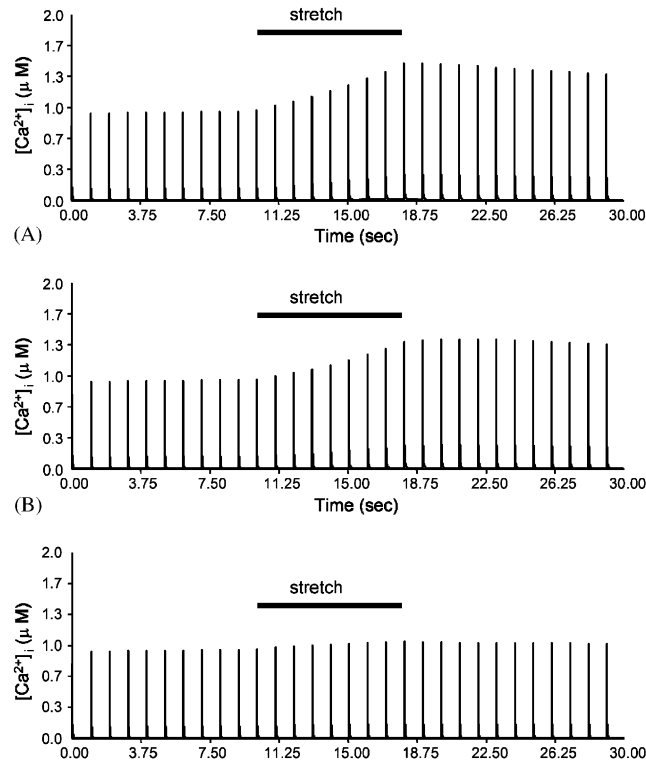


Fig. 5. Model predictions of changes in Ca^{2+} transients by activation of SACs (corresponding to a 10% stretch) with different ionic permeabilities. (A) A prediction of changes in Ca^{2+} transients when $P_{\text{Na}^+}:P_{\text{K}^+}:P_{\text{Ca}^{2+}}$ through SACs is 1:1.32:0.70. (B) A prediction of changes in Ca^{2+} transients when $P_{\text{Ca}^{2+}}$ is 0 ($P_{\text{Na}^+}:P_{\text{K}^+}:P_{\text{Ca}^{2+}} = 1:1.32:0$). (C) A prediction of changes in Ca^{2+} transients when P_{Na^+} is 0 ($P_{\text{Na}^+}:P_{\text{K}^+}:P_{\text{Ca}^{2+}} = 0:1.32:0.7$). The stimulus interval was 1.0 s.

axis were found to follow the time course of $[\text{Na}^+]_i$ (Fig. 6B), which further supports the idea that the gradual increase in the amplitude of Ca^{2+} transients during a stretch has an association with an indirect pathway related to the increase in Na^+ influx through SACs. We tested this idea by making $[\text{Na}^+]_i$ unchanged during the stretch or by removing the $[\text{Na}^+]_i$ -dependent activation of the $\text{Na}^+/\text{Ca}^{2+}$ exchanger using the model simulation. As shown in Fig. 7B, making $[\text{Na}^+]_i$ constant markedly attenuated the stretch-induced changes in the Ca^{2+} transients. Removing the $[\text{Na}^+]_i$ -dependent activation of the $\text{Na}^+/\text{Ca}^{2+}$ exchanger also reduced the stretch-induced changes in the Ca^{2+} transients (Fig. 7C).

4. Discussion

The objectives of the present study were to reproduce the stretch-induced changes of rat atrial myocytes and to study the role of SACs in these changes using a model simulation. The experimental part of the study demonstrated that a stretch increases membrane conductance and

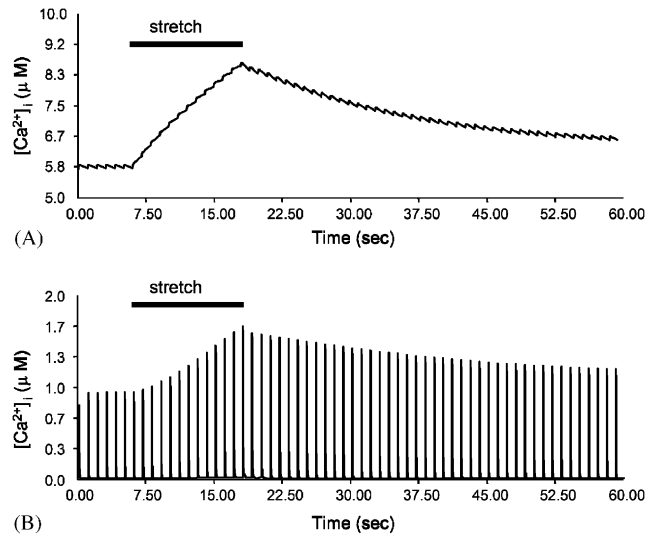


Fig. 6. Model predictions of $[Na^+]_i$ (A) and Ca^{2+} transients (B) during application and release of stretch (10% stretch). The stimulus interval was 1.0 s.

shifts the reversal potential to the positive direction. The study also demonstrated that the stretch depolarises the diastolic membrane and prolongs the APD, which are thought to be produced by the opening of the SACs. A relationship between the extent of the stretch and the opening of the SACs was then formulated and included in the model simulation to perform a modelling study. The modelling part of the study demonstrated that introducing the SACs into the model successfully reproduces the stretch-induced changes of the AP, such as diastolic depolarisation and APD prolongation, obtained from the experimental part of the study. The modelling part of the study also suggested that the opening of SACs during a sustained stretch makes the Ca^{2+} transients bigger. Finally, the model predicted that the influx of Na^+ rather than Ca^{2+} through SACs has a more crucial role in the development of these stretch-induced changes in the AP or Ca^{2+} transients.

The I_{SAC} induced by the stretch in the rat atrial myocytes showed a nearly linear voltage dependence and reversed polarity near -6 mV under physiological ionic conditions. I_{SAC} has also been analysed with a similar technique in the ventricular cells of humans (Kamkin et al., 2000), guinea-pigs (Sasaki et al., 1992; Kamkin et al., 2000; Calaghan et al., 2003), rats (Kamkin et al., 2000), mice (Kamkin et al., 2003), and frogs (Riemer and Tung, 2003). In most cases, I_{SAC} showed a voltage dependence and reversal potential similar to our results. I_{SAC} is thought to act as an outward current at positive potentials and an inward current at negative potentials because the reversal potential of the I_{SAC} is near 0 mV. Therefore, the activation of the I_{SAC} can speed up early repolarisation and retard late repolarisation. In addition, the activation of the I_{SAC} should depolarise the diastolic cell membrane because the stretch shifts the currents to more negative values at negative potentials. In agreement with this idea, the activation of the I_{SAC} , in both the model simulation and the real experiment, decreased the APD at positive potentials and increased

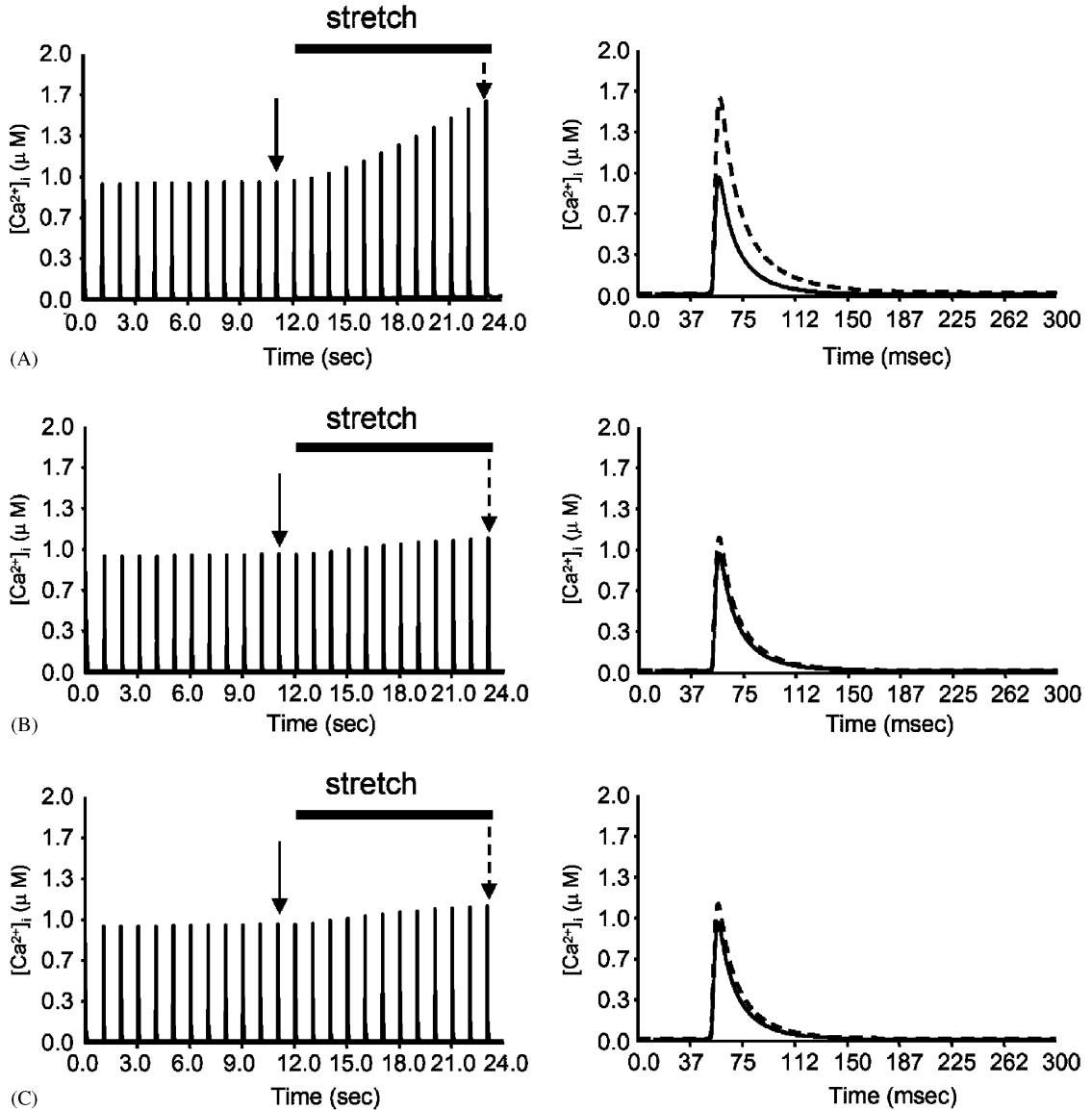


Fig. 7. Model predictions of changes in Ca^{2+} transients under (A) control conditions, (B) constant $[Na^+]_i$ (5.4 mM), and (C) removal of $[Na^+]_i$ -dependent activation of the Na^+/Ca^{2+} exchanger during the stretch (10% stretch). Each trace in the right panel (solid: redrawn from the point indicated by solid arrows in the left panel; dotted: redrawn from the point indicated by dotted arrows) denotes the expanded Ca^{2+} transients. The stimulus interval was 1.0 s.

it at negative potentials: thus, the two APs crossed over (Fig. 3). In guinea-pig ventricular myocytes, a direct stretch induced diastolic depolarisation and AP prolongation (Kamkin et al., 2000), which agrees with our results. Calaghan et al. (2003) also found that the direct stretch of guinea-pig ventricular myocytes prolonged the APD. However, there are contradictory reports on

the effect of stretch on the APD (White et al., 1993; Tung and Zou, 1995), showing that a stretch decreased the APD. The discrepancy seems to result from the different definitions of APD used in each study. If one determines APD at early repolarisation, the response to stretch should be recognised as a decrease in APD, while the response is regarded as an increase when determined at late repolarisation. The acceleration of early repolarisation by a stretch is noteworthy in that it reduces the refractory period, which favours a pro-arrhythmic condition (Wijffels et al., 1997; Franz and Bode, 2003).

When the extent of stretch-induced diastolic membrane depolarisation reached a threshold, APs were triggered without electrical stimulation in both the model simulation and the real experiment (Fig. 3). The stretch-induced premature APs have also been shown in the papillary muscle of a Rhesus monkey (Kaufmann and Theophile, 1967) and in the rat atrium (Kamkin et al., 2000). These results strongly suggest the pro-arrhythmic effect of an excessive I_{SAC} (Stacy et al., 1992). The involvement of SACs in the stretch-induced vulnerability to atrial arrhythmia was demonstrated by using the specific SAC blocker isolated from the venom of the tarantula *Grammostola spatulata* (Bode et al., 2001).

The stretch of the intact heart, isolated muscle, and single myocyte causes an immediate increase in force owing to an increase in myofilament Ca^{2+} sensitivity, followed by a secondary and slower increase in force that takes place over several minutes (Parmley and Chuck, 1973; Tucci et al., 1984). Allen and Kurihara (1982) showed that the slow response is associated with a corresponding increase in the magnitude of the Ca^{2+} transients. The increase in the magnitude of the Ca^{2+} transients produced by a stretch has been clearly demonstrated in the rat atrium (Tavi et al., 1998) and isolated rat ventricular trabeculae (Kentish and Wrzosek, 1998; Alvarez et al., 1999). Our model simulation agreed with these results and also demonstrated an increase in the amplitude of Ca^{2+} transients during a stretch (Fig. 5). The underlying mechanism of the stretch-induced changes in Ca^{2+} transients, however, still remains to be explained. In order to explain the gradual increase of Ca^{2+} transients during a stretch, the possible pathway of Ca^{2+} influx must be discussed. Primarily, Ca^{2+} influx through SACs must be discussed. The majority of SACs have considerable permeability for both monovalent and divalent cations (Sachs, 1988; Kim, 1993). Our model of SACs also has permeability for Ca^{2+} and Na^+ . Thus, the activation of SACs should lead to an increase in the amplitude of the Ca^{2+} transients. Our model simulation, however, suggested that the permeability for Na^+ rather than Ca^{2+} is the major trigger for the stretch-induced change in Ca^{2+} transients (Fig. 4). Although Ca^{2+} influx through SACs is also noticeable, it is unlikely that this is the major pathway of Ca^{2+} influx during a stretch. As a second possibility, Ca^{2+} influx through the L-type Ca^{2+} current ($I_{Ca,L}$) should be discussed. Although the major Ca^{2+} influx pathway during an AP is the L-type Ca^{2+} current ($I_{Ca,L}$) in the cardiac cell, this possibility is also unlikely given the results that an axial stretch caused no increase in $I_{Ca,L}$ in guinea-pig, ferret, and rat myocytes (Sasaki et al., 1992; Hongo et al., 1996; Kamkin et al., 2000; Belus and White, 2003). However, there is a possibility that extra Ca^{2+} might enter the cell via $I_{Ca,L}$ and partly contribute to the increase in the amplitude of Ca^{2+} transients owing to delayed voltage-dependent inactivation during the prolonged depolarisation (Calaghan et al., 2003; Kamkin et al., 2003). Finally, an increase in Ca^{2+} influx through the Na^+/Ca^{2+} exchanger operating in a reverse-mode could be possible. Our model predicted that the activation of SACs could increase the amplitude of Ca^{2+} transients indirectly. The influx of Na^+ through the SACs is thought to induce Na^+ accumulation in the cytosol, as SACs are permeable to Na^+ .

There is evidence that a stretch increases the cytosolic and total Na^+ concentration in human, mouse, and rat ventricular myocytes (Alvarez et al., 1999; Baartscheer et al., 2003; Isenberg et al., 2003). Na^+ accumulation favours the reverse-mode operation of the $\text{Na}^+/\text{Ca}^{2+}$ exchanger during the rising phase of the AP (Alvarez et al., 1999; Perez et al., 2001; Calaghan et al., 2003). The increase in Ca^{2+} influx through the $\text{Na}^+/\text{Ca}^{2+}$ exchanger could then make the Ca^{2+} transients bigger during the stretch. In support of the above explanation for the underlying mechanism, making $[\text{Na}^+]_i$ unchanged during the stretch or removing the $[\text{Na}^+]_i$ -dependent activation of the $\text{Na}^+/\text{Ca}^{2+}$ exchanger in the model produced a marked decrease in the stretch-induced changes in the Ca^{2+} transients (Fig. 7C).

The results concerning the stretch-induced change of the diastolic $[\text{Ca}^{2+}]_i$ are controversial. Some studies do show an increase in the diastolic $[\text{Ca}^{2+}]_i$ (White et al., 1993; Gannier et al., 1994, 1996), which agrees with our findings. However, there are conflicting studies that show that the diastolic $[\text{Ca}^{2+}]_i$ does not change during the stretch (Hongo et al., 1996; Tavi et al., 1998). The contradictory data in the literature may be explained by considering that a moderate increase of Ca^{2+} influx is well counterbalanced by the $\text{Na}^+/\text{Ca}^{2+}$ exchanger or plasmalemma Ca^{2+} pump, whereas a severe increase in Ca^{2+} influx eventually leads to Ca^{2+} accumulation, elevating diastolic $[\text{Ca}^{2+}]_i$. The exact influence and role of a stretch on the diastolic $[\text{Ca}^{2+}]_i$ remain to be studied.

The model simulation of the present study faithfully reproduced the stretch-induced changes in APs and Ca^{2+} transients of rat atrial myocytes and also provided insight into the possible role of SACs in the stretch-induced changes and the underlying mechanism. The Na^+ influx via the SACs not only changes the shape of APs, but also augments the Ca^{2+} transients most probably via a reverse-mode operation of the $\text{Na}^+/\text{Ca}^{2+}$ exchangers. The further investigation about the stretch-induced modulation of various ion channels in cardiac myocytes and the incorporation of those parameters would improve the model prediction of the cardiac electrophysiology.

Editor's note

Please see also related communications in this volume by Sobie et al. (2005) and Cooper et al. (2005). For further downloadable content please see <http://www.physiome.org.nz/publications/PBMB-2005-89/Youm/>

Acknowledgements

This work was supported in part by funds from the Advanced Backbone IT Technology Development Project of the Ministry of Information and Communication (IMT-2000-C3-5; IMT-2000-C3-3) and a Non-Directed Research Fund from the Korea Research Foundation (1996). We would like to thank Drs. A. Noma, N. Sarai, and S. Matsuoka for introducing the Kyoto model to us.

Appendix

Parameter details and definition of symbols are given in Tables 1 and 2.

Table 1

Parameter details

Cell geometry:

Cell volume: $V_i = 4046 \mu\text{m}^3$ SR release site: $V_{\text{rel}} = 0.02 V_i \mu\text{m}^3$ SR uptake site: $V_{\text{up}} = 0.05 V_i \mu\text{m}^3$ Membrane capacitance: $C_m = 50 \text{ pF}$

Ionic concentrations used:

 $[\text{K}^+]_i = 140 \text{ mM}$ $[\text{Na}^+]_i = 5.4 \text{ mM}$ $[\text{Ca}^{2+}]_i = 3.5 \text{ nM}$ $[\text{K}^+]_o = 5.4 \text{ mM}$ $[\text{Na}^+]_o = 140 \text{ mM}$ $[\text{Ca}^+]_o = 1.8 \text{ mM}$

Table 2

Definition of symbols

Inward rectifier K^+ channel: I_{K1} : inward rectifier K^+ current

C: closed state

O: open state

B: blocked state

 n : activation gate f_B : fraction of block f_U : fraction of unblock α_n and β_n : opening and closing rate constants, respectively, ms^{-1} μ : rate constant of block, ms^{-1} λ : rate constant of unblock, ms^{-1}

Depolarisation-activated outward channel:

 $I_{\text{K,out}}$: depolarisation-activated outward K^+ current $I_{\text{K,fast}}$: fast component of depolarisation-activated outward K^+ current $I_{\text{K,slow}}$: slow component of depolarisation-activated outward K^+ current m, h : activation and inactivation gates, respectively α_m and β_m : opening and closing rate constants, respectively, of activation gate, ms^{-1} α_h and β_h : opening and closing rate constants, respectively, of inactivation gate, ms^{-1} F : Faraday constant, $96.4867 \text{ C mmol}^{-1}$ R : gas constant, $8.3143 \text{ C mV K}^{-1} \text{ mmol}^{-1}$ T : absolute temperature, 298.15 K V : membrane potential, mV E_K : reversal potential of K^+ , mV

References

- Allen, D.G., Kurihara, S., 1982. The effects of muscle length on intracellular calcium transients in mammalian cardiac muscle. *J. Physiol.* 327, 79–94.
- Alvarez, B.V., Perez, N.G., Ennis, I.L., Camilion de Hurtado, M.C., Cingolani, H.E., 1999. Mechanisms underlying the increase in force and Ca^{2+} transient that follow stretch of cardiac muscle: a possible explanation of the Anrep effect. *Circ. Res.* 85, 716–722.

- Baartscheer, A., Schumacher, C.A., Belterman, C.N., Coronel, R., Fiolet, J.W., 2003. $[\text{Na}^+]_i$ and the driving force of the $\text{Na}^+/\text{Ca}^{2+}$ -exchanger in heart failure. *Cardiovasc. Res.* 57, 986–995.
- Belus, A., White, E., 2003. Streptomycin and intracellular calcium modulate the response of single guinea-pig ventricular myocytes to axial stretch. *J. Physiol.* 546, 501–509.
- Bode, F., Sachs, F., Franz, M.R., 2001. Tarantula peptide inhibits atrial fibrillation. *Nature* 409, 35–36.
- Boland, J., Troquet, J., 1980. Intracellular action potential changes induced in both ventricles of the rat by an acute right ventricular pressure overload. *Cardiovasc. Res.* 14, 735–740.
- Boyle, W.A., Nerbonne, J.M., 1992. Two functionally distinct 4-aminopyridine-sensitive outward K^+ currents in rat atrial myocytes. *J. Gen. Physiol.* 100, 1041–1067.
- Brady, A.J., 1991. Mechanical properties of isolated cardiac myocytes. *Physiol. Rev.* 71, 413–428.
- Bustamante, J.O., Ruknudin, A., Sachs, F., 1991. Stretch-activated channels in heart cells: relevance to cardiac hypertrophy. *J. Cardiovasc. Pharmacol.* 17, S110–S113.
- Calaghan, S.C., Belus, A., White, E., 2003. Do stretch-induced changes in intracellular calcium modify the electrical activity of cardiac muscle? *Prog. Biophys. Mol. Biol.* 82, 81–95.
- Casadei, B., Sears, C.E., 2003. Nitric oxide mediated regulation of cardiac contractility and stretch responses. *Prog. Biophys. Mol. Biol.* 82, 67–80.
- Cazorla, O., Pascrel, C., Brette, F., Le Guennec, J.Y., 1999. Modulation of ions channels and membrane receptors activities by mechanical interventions in cardiomyocytes: possible mechanisms for mechanosensitivity. *Prog. Biophys. Mol. Biol.* 71, 29–58.
- Cooper et al., 2005. Soft tissue impact characterisation kit (STICK) for ex situ investigation of heart rhythm responses to acute mechanical stimulation. *Prog. Biophys. Mol. Biol.*, this issue.
- Craelius, W., 1993. Stretch-activation of rat cardiac myocytes. *Exp. Physiol.* 78, 411–423.
- Dean, J.W., Lab, M.J., 1989. Arrhythmia in heart failure: role of mechanically induced changes in electrophysiology. *Lancet* 1, 1309–1312.
- Franz, M.R., Bode, F., 2003. Mechano-electrical feedback underlying arrhythmias: the atrial fibrillation case. *Prog. Biophys. Mol. Biol.* 82, 163–174.
- Franz, M.R., Burkhoff, D., Yue, D.T., Sagawa, K., 1989. Mechanically induced action potential changes and arrhythmia in isolated and in situ canine hearts. *Cardiovasc. Res.* 23, 213–223.
- Franz, M.R., Cima, R., Wang, D., Profitt, D., Kurz, R., 1992. Electrophysiological effects of myocardial stretch and mechanical determinants of stretch-activated arrhythmias [published erratum appears in *Circulation* 1992;86:1663]. *Circulation* 86, 968–978.
- Gannier, F., White, E., Lacampagne, A., Garnier, D., Le Guennec, J.Y., 1994. Streptomycin reverses a large stretch induced increases in $[\text{Ca}^{2+}]_i$ in isolated guinea pig ventricular myocytes. *Cardiovasc. Res.* 28, 1193–1198.
- Gannier, F., White, E., Garnier, D., Le Guennec, J.Y., 1996. A possible mechanism for large stretch-induced increase in $[\text{Ca}^{2+}]_i$ in isolated guinea-pig ventricular myocytes. *Cardiovasc. Res.* 32, 158–167.
- Hamill, O.P., Marty, A., Neher, E., Sakmann, B., Sigworth, F.J., 1981. Improved patch-clamp techniques for high-resolution current recording from cells and cell-free membrane patches. *Pflugers Arch.* 391, 85–100.
- Hansen, D.E., 1993. Mechanoelectrical feedback effects of altering preload, afterload, and ventricular shortening. *Am. J. Physiol.* 264, H423–H432.
- Hansen, D.E., Borganelli, M., Stacy Jr., G.P., Taylor, L.K., 1991. Dose-dependent inhibition of stretch-induced arrhythmias by gadolinium in isolated canine ventricles. Evidence for a unique mode of antiarrhythmic action. *Circ. Res.* 69, 820–831.
- Hongo, K., White, E., Le Guennec, J.Y., Orchard, C.H., 1996. Changes in $[\text{Ca}^{2+}]_i$, $[\text{Na}^+]_i$ and Ca^{2+} current in isolated rat ventricular myocytes following an increase in cell length. *J. Physiol.* 491, 609–619.
- Hoyer, J., Distler, A., Haase, W., Gogelein, H., 1994. Ca^{2+} influx through stretch-activated cation channels activates maxi K^+ channels in porcine endocardial endothelium. *Proc. Natl. Acad. Sci. USA* 91, 2367–2371.
- Hu, H., Sachs, F., 1996. Mechanically activated currents in chick heart cells. *J. Membr. Biol.* 154, 205–216.
- Isenberg, G., Borschke, B., Rueckschloss, U., 2003. Ca^{2+} transients of cardiomyocytes from senescent mice peak late and decay slowly. *Cell Calcium* 34, 271–280.
- Kamkin, A., Kiseleva, I., Isenberg, G., 2000. Stretch-activated currents in ventricular myocytes: amplitude and arrhythmogenic effects increase with hypertrophy. *Cardiovasc. Res.* 48, 409–420.

- Kamkin, A., Kiseleva, I., Isenberg, G., 2003. Ion selectivity of stretch-activated cation currents in mouse ventricular myocytes. *Pflugers Arch.* 446, 220–231.
- Kaufmann, R., Theophile, U., 1967. Autonomously promoted extension effect in Purkinje fibers, papillary muscles and trabeculae carnae of rhesus monkeys. *Pflugers Arch. Gesamte. Physiol. Menschen. Tiere.* 297, 174–189.
- Kentish, J.C., Wrzosek, A., 1998. Changes in force and cytosolic Ca^{2+} concentration after length changes in isolated rat ventricular trabeculae. *J. Physiol.* 506, 431–444.
- Kim, D., 1993. Novel cation-selective mechanosensitive ion channel in the atrial cell membrane. *Circ. Res.* 72, 225–231.
- Kiseleva, I., Kamkin, A., Wagner, K.D., Theres, H., Ladhoff, A., Scholz, H., Gunther, J., Lab, M.J., 2000. Mechanoelectric feedback after left ventricular infarction in rats. *Cardiovasc. Res.* 45, 370–378.
- Kohl, P., Ravens, U., 2003. Cardiac mechano-electric feedback: past, present, and prospect. *Prog. Biophys. Mol. Biol.* 82, 3–9.
- Kohl, P., Hunter, P., Noble, D., 1999. Stretch-induced changes in heart rate and rhythm: clinical observations, experiments and mathematical models. *Prog. Biophys. Mol. Biol.* 71, 91–138.
- Lab, M.J., 1978. Mechanically dependent changes in action potentials recorded from the intact frog ventricle. *Circ. Res.* 42, 519–528.
- Lab, M.J., 1982. Contraction-excitation feedback in myocardium. Physiological basis and clinical relevance. *Circ. Res.* 50, 757–766.
- Lab, M.J., 1996. Mechanoelectric feedback (transduction) in heart: concepts and implications. *Cardiovasc. Res.* 32, 3–14.
- Matsuoka, S., Sarai, N., Kuratomi, S., Ono, K., Noma, A., 2003. Role of individual ionic current systems in ventricular cells hypothesized by a model study. *Jpn. J. Physiol.* 53, 105–123.
- Nazir, S.A., Lab, M.J., 1996. Mechanoelectric feedback in the atrium of the isolated guinea-pig heart. *Cardiovasc. Res.* 32, 112–119.
- Niu, W., Sachs, F., 2003. Dynamic properties of stretch-activated K^+ channels in adult rat atrial myocytes. *Prog. Biophys. Mol. Biol.* 82, 121–135.
- Parmley, W.W., Chuck, L., 1973. Length-dependent changes in myocardial contractile state. *Am. J. Physiol.* 224, 1195–1199.
- Perez, N.G., De Hurtado, M.C.C., Cingolani, H.E., 2001. Reverse mode of the $\text{Na}^+ - \text{Ca}^{2+}$ exchange after myocardial stretch: underlying mechanism of the slow force response. *Circ. Res.* 88, 376–382.
- Petroff, M.G.V., Kim, S.H., Pepe, S., Dessy, C., Marban, E., Balligand, J-L., Sollott, S.J., 2001. Endogenous nitric oxide mechanisms mediate the stretch dependence of Ca^{2+} release in cardiomyocytes. *Nat. Cell Biol.* 3, 867–873.
- Riemer, T.L., Tung, L., 2003. Stretch-induced excitation and action potential changes of single cardiac cells. *Prog. Biophys. Mol. Biol.* 82, 97–110.
- Sachs, F., 1988. Mechanical transduction in biological systems. *Crit. Rev. Biomed. Eng.* 16, 141–169.
- Sachs, F., 1994. Modeling mechanical-electrical transduction in the heart. In: Mow, V.C., Guliak, F., Trans-Son-Tray, R., Hochmuth, R.M. (Eds.), *Cell Mechanics and Cellular Engineering*. Springer, New York, pp. 308–328.
- Sarai, N., Matsuoka, S., Kuratomi, S., Ono, K., Noma, A., 2003. Role of individual ionic current systems in the SA node hypothesized by a model study. *Jpn. J. Physiol.* 53, 125–134.
- Sasaki, N., Mitsuiye, T., Noma, A., 1992. Effects of mechanical stretch on membrane currents of single ventricular myocytes of guinea-pig heart. *Jpn. J. Physiol.* 42, 957–970.
- Sorota, S., 1992. Swelling-induced chloride-sensitive current in dog atrial cells revealed by whole-cell patch clamp method. *Circ. Res.* 70, 679–687.
- Stacy Jr., G.P., Jobe, R.L., Taylor, L.K., Hansen, D.E., 1992. Stretch-induced depolarizations as a trigger of arrhythmias in isolated canine left ventricles. *Am. J. Physiol.* 263, H613–H621.
- Taggart, P., 1996. Mechano-electric feedback in the human heart. *Cardiovasc. Res.* 32, 38–43.
- Tavi, P., Han, C., Weckstrom, M., 1998. Mechanisms of stretch-induced changes in $[\text{Ca}^{2+}]_i$ in rat atrial myocytes: role of increased troponin C affinity and stretch-activated ion channels. *Circ. Res.* 83, 1165–1177.
- Terrenoire, C., Lauritzen, I., Lesage, F., Romey, G., Lazdunski, M., 2001. A TREK-1-like potassium channel in atrial cells inhibited by beta-adrenergic stimulation and activated by volatile anesthetics. *Circ. Res.* 89, 336–342.
- Tseng, G.N., 1992. Cell swelling increases membrane conductance of canine cardiac cells: evidence for a volume-sensitive Cl channel. *Am. J. Physiol.* 262, C1056–C1068.

- Tucci, P.F.J., Bregagnollo, E.A., Spadaro, J., Cicogna, A.C., Ribeiro, M.C.L., 1984. Length dependence of activation studied in the isovolumic blood-perfused dog heart. *Circ. Res.* 55, 59–66.
- Tung, L., Zou, S., 1995. Influence of stretch on excitation threshold of single frog ventricular cells. *Exp. Physiol.* 80, 221–235.
- Vandenberg, J., Yoshida, A., Kirk, K., Powell, T., 1994. Swelling-activated and isoprenaline-activated chloride currents in guinea pig cardiac myocytes have distinct electrophysiology and pharmacology. *J. Gen. Physiol.* 104, 997–1017.
- White, E., Le Guennec, J.Y., Nigretto, J.M., Gannier, F., Argibay, J.A., Garnier, D., 1993. The effects of increasing cell length on auxotonic contractions; membrane potential and intracellular calcium transients in single guinea-pig ventricular myocytes. *Exp. Physiol.* 78, 65–78.
- Wijffels, M.C., Kirchhof, C.J., Dorland, R., Power, J., Allessie, M.A., 1997. Electrical remodeling due to atrial fibrillation in chronically instrumented conscious goats: roles of neurohumoral changes, ischemia, atrial stretch, and high rate of electrical activation. *Circulation* 96, 3710–3720.
- Youm, J.B., Ho, W.K., Earm, Y.E., 2000. Permeability characteristics of monovalent cations in atrial myocytes of the rat heart. *Exp. Physiol.* 85, 143–150.
- Zeng, T., Bett, G.C.L., Sachs, F., 2000. Stretch-activated whole cell currents in adult rat cardiac myocytes. *Am. J. Physiol.* 278, H548–H557.
- Zhang, Y.H., Youm, J.B., Sung, H.K., Lee, S.H., Ryu, S.Y., Ho, W.K., Earm, Y.E., 2000. Stretch-activated and background non-selective cation channels in rat atrial myocytes. *J. Physiol.* 523, 607–619.

Further reading

- Brown, H.F., DiFrancesco, D., Noble, S.J., 1979. How does adrenaline accelerate the heart? *Nature* 280, 236.
- Dale, H.H., 1954. The beginnings and prospects of neurohumoral transmission. *Pharmacol. Rev.* 6, 7–13.
- Kohl, P., 2003. Heterogeneous cell coupling in the heart: an electrophysiological role for fibroblasts. *Circ. Res.* 93, 381–383.
- Noma, A., Irisawa, H., 1976. Membrane currents in the rabbit sinoatrial node cell as studied by the double microelectrode method. *Pflugers Arch.* 364, 45–52.